

Electronic Supplementary Material (ESI) for Journal of Materials Chemistry C.
This journal is © The Royal Society of Chemistry 2024

**New Insight on π - π Interactions: Realization of Full Color Emission from
Blue to Red under Hydrostatic Pressure without Exogenous Intramolecular
Charge Transfer**

Aisen Li,^[a, b] Jiaqiang Wang,^[d] Changjiang Bi,^[e] Zirun Chen,^[b] Shuping Xu,^[e] Kai Wang,^[b] Jinfeng
Wang,^{*[c]} and Zhen Li^{*[a, c, d]}

Affiliations:

[a] Joint School of National University of Singapore and Tianjin University, International Campus
of Tianjin University, Binhai New City, Fuzhou 350207, China

[b] School of Physical Science and Information Technology, Liaocheng University, Liaocheng
252059, China

[c] Institute of Molecular Aggregation Science, Tianjin University, Tianjin 300072, China

[d] Hubei Key Lab on Organic and Polymeric Opto-Electronic Materials, Department of Chemistry,
Wuhan University, Wuhan 430072, China

[e] State Key Laboratory of Supramolecular Structure and Materials, Institute of Theoretical
Chemistry, College of Chemistry, Jilin University, Changchun 130012, China

Contents

1. Experimental Section	3
2. XRD patterns of X2EP-B and X2EP-N.....	5
3. PL spectra of Pyrene and X2P.....	6
3. Calculated results of Pyrene and X2P.....	7
4. Calculated results of X2EP-N.....	11
5. PL spectra of X2EP-B and X2EP-N during decompression process	17
6. Analysis on π - π overlap and distance of X2EP-N.....	18
7. Analysis on stacking mode of Pyrene, X2P and X2EP-B.....	21
8. Lifetime of X2EP-N and X2EP-B.....	22
9. PL spectra of X2EP-N during the second compression.	23
10. Absorption of X2EP-B and X2EP-N during compression process.....	24
11. References.....	25

1. Experimental Section

Preparation of Sample

Pyrene was purchased from Sigma-Aldrich (Analytical Standard) and the corresponding single crystal was obtained from the mixed solution of tetrahydrofuran/n-hexane. X2P and X2EP crystals were cultured as we reported previously.^[1]

Experimental Measurements.

The high-pressure experiments were performed by a diamond anvil cell (DAC) with a diameter of 350 μm at room temperature. The prepared sample was loaded into the sample chamber with a diameter of 200 μm on a T301 stainless steel gasket ($d=5.00$ mm). Meanwhile, a small ruby chip was added into the same hole along with the sample for in situ pressure-calibration according to monitoring the fluorescence band shift of R1 line. And in order to guarantee for obtaining the hydrostatic pressure according to the Pascal's principle, silicone oil was added as a pressure-transmitting medium (PTM). A Horiba Jobin Yvon T64000 model Raman spectrometer equipped with an argon laser source of 532 nm and a holographic grating of 1800 gr/mm, was used to collect the ruby signal and perform pressure-calibration. Additionally, the high-pressure emission spectra under nonhydrostatic and hydrostatic conditions were measured through a fluorescence microscope (IX71, Olympus 20 \times , numerical aperture=0.4) equipped with a spectrometer (Horiba Jobin Yvon iHR320) and a mercury lamp (an excitation wavelength of 365 nm). High-pressure UV-Visible absorption spectra were measured with an QE65 Pro high-sensitivity spectrometer using a DH-2000-BAL light source (UV-VIS-NIR, deuterium and halogen). The corresponding optical photographs were recorded by an imaging camera (EOS 5D Mark IV) with an xenon cold light source. Time-Resolved PL Measurements were performed by FLS1000 (Edinburgh) coupled with the homemade optical path, and the excitation wavelength is 375 nm.

Computational Methods.

Theoretical calculation of molecular structures and stacking mode at different pressure values was carried out based on the unit cell information by using the CASTEP package in Material Studio 7.0. This calculation was performed using Norm-conserving pseudopotentials with 750 eV energy cutting off. The initial stacking modes and geometries was fully relaxed under external stress values of 0, 1.0, 2.0, 3.0, 4.0, 5.0, 6.0, 7.0, 8.0, 9.0 and 10.0 GPa. The generalized gradient

approximation (GGA) with Perdew Burke Ernzerhof (PBE) was applied to describe the exchange-correlation (XC) effects. TS scheme was used for dispersion corrections. All the calculations about excited states were performed with density functional theory (DFT) and time-dependent density functional theory (TDDFT) with B3LYP/6-31G(d) method implemented in Gaussian 09 program package. Independent gradient model based on Hirshfeld partition (IGMH) analysis of X2EP-N was performed and the calculated models were established by extracting molecules from the cell structures at different pressures. The cubic files (.cub) for IGMH analysis were generated by the wavefunction software Multiwfn 3.8,^[2-4] and the IGMH inter surfaces were visualized and analysed using the Visual Molecular Dynamics program (VMD 1.93).^[5]

2. XRD patterns of X2EP-B and X2EP-N

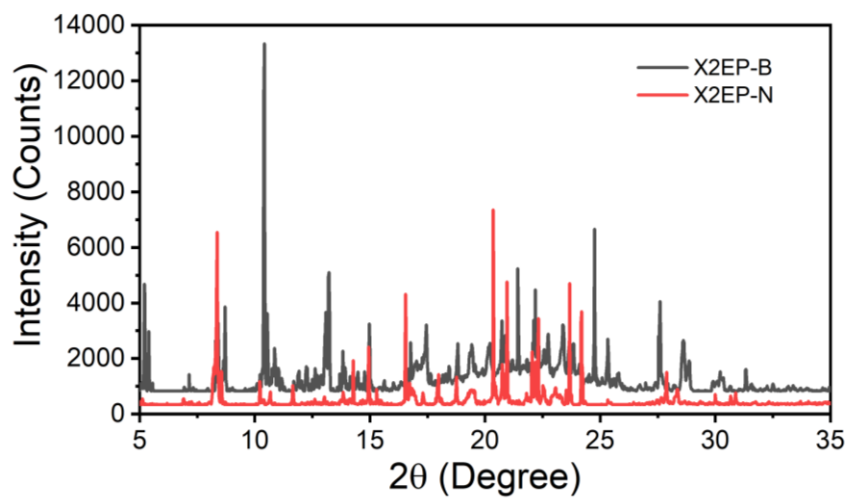


Figure S1. The XRD patterns of X2EP-B and X2EP-N, respectively.

3. PL spectra of Pyrene and X2P

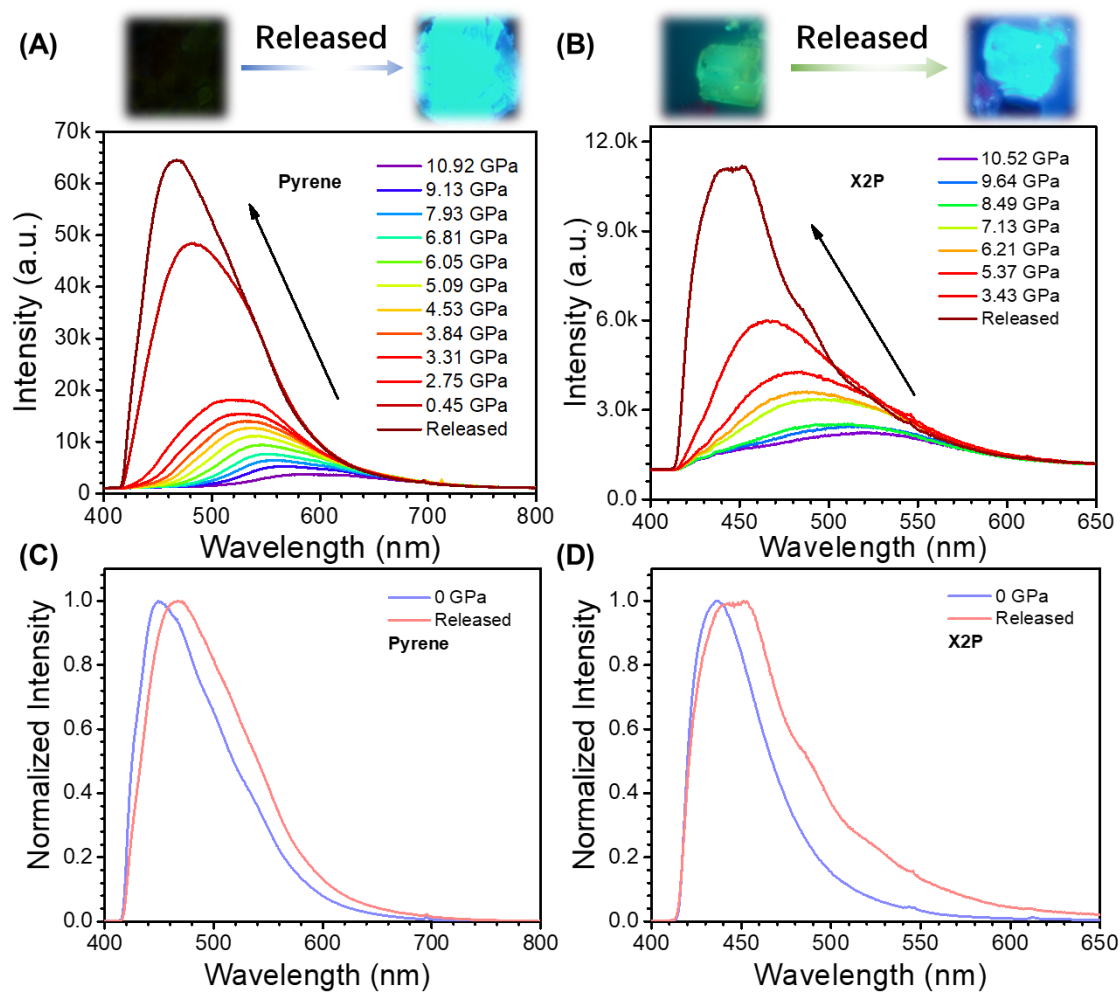


Figure S2. The PL spectra of pyrene (A) and X2P (B) during the decompression process; The comparison between recovered spectrum and initial state of pyrene (C) and X2P (D).

3. Calculated results of Pyrene and X2P

Table S1. The crystal parameters of Pyrene at different pressure values calculated by Materials Studio 2017.

Stress	a/Å	b/Å	c/Å	$\alpha/^\circ$	$\beta/^\circ$	$\gamma/^\circ$	$v/\text{Å}^3$
Exp. Data	8.4539	9.2511	13.612	90	100.386	90	1047.1
0 GPa	9.0044	11.3431	14.0677	90	101.7818	90	1061.08
1.0 GPa	8.5224	9.2433	13.7403	90	101.3895	90	978.58
2.0 GPa	8.2117	9.0555	13.3765	90	100.3275	90	928.77
3.0 GPa	8.1092	8.7984	13.2130	90	99.8688	90	891.13
4.0 GPa	8.0248	8.5980	13.1003	90	99.6371	90	862.42
5.0 GPa	7.9856	8.4915	12.9238	90	100.2319	90	839.74
6.0 GPa	7.9429	8.3366	12.8807	90	100.0849	90	819.28
7.0 GPa	7.8943	8.2247	12.8083	90	99.8833	90	801.77
8.0 GPa	7.8539	8.1242	12.7509	90	99.7810	90	801.77
9.0 GPa	7.8198	8.0305	12.7067	90	99.75179	90	786.41
10.0 GPa	7.7874	7.9518	12.6570	90	99.7267	90	772.50

Table S2. The crystal parameters of X2P at different pressure values calculated by Materials Studio 2017.

Stress	a/Å	b/Å	c/Å	$\alpha/^\circ$	$\beta/^\circ$	$\gamma/^\circ$	$V/\text{Å}^3$
Exp. Data	9.256	24.763	17.376	90	95.953	90	3961
0 GPa	9.9023	25.8649	18.3450	90	92.9503	90	4692.33
1.0 GPa	9.2191	24.9052	17.5570	90	97.4375	90	3997.23
2.0 GPa	8.9524	24.2551	17.1299	90	99.1267	90	3672.52
3.0 GPa	8.7306	24.2107	16.6777	90	100.2325	90	3469.16
4.0 GPa	8.6006	24.0010	16.4868	90	101.0059	90	3340.66
5.0 GPa	8.4985	23.8448	16.3299	90	101.4845	90	3242.92
6.0 GPa	8.4624	23.5782	16.1446	90	101.7362	90	3153.96
7.0 GPa	8.4025	23.4639	16.0750	90	101.9324	90	3100.79
8.0 GPa	8.3148	23.4366	15.7867	90	101.7330	90	3012.09
9.0 GPa	8.2612	23.3069	15.7118	90	102.0434	90	2958.61
10.0 GPa	8.2145	23.1794	15.6227	90	102.2361	90	2907.10

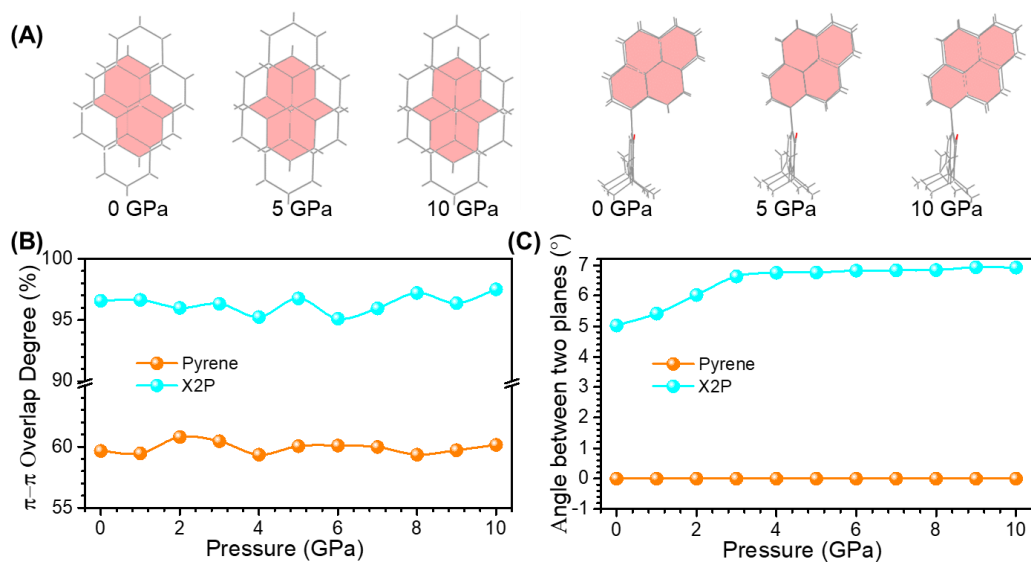


Figure S3. The analysis of π - π overlap degree between two pyrene planes of pyrene and X2P based on the calculated results: (A) photograph and (B) variation trend with the increased pressure; (C) The variation trend of angle between two planes at different pressure.

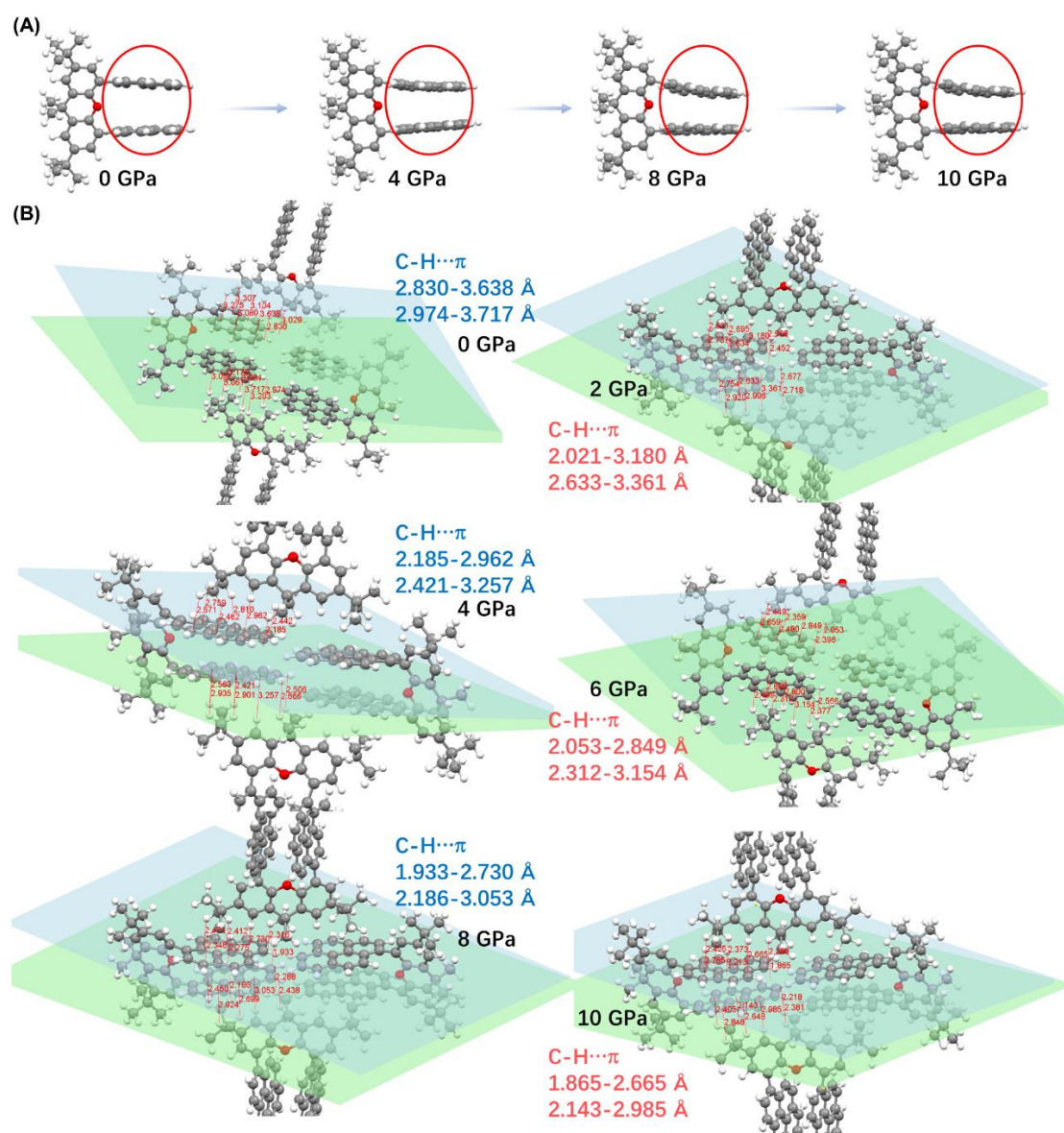


Figure S4. The changes of molecular structure (A) and intermolecular interactions (C-H... π on pyrene units) (B) of X2P with the increased pressure from calculated results.

4. Calculated results of X2EP-N

Table S3. The crystal parameters of X2EP-N at different pressure values calculated by Materials Studio 2017.

Stress	a/Å	b/Å	c/Å	$\alpha/^\circ$	$\beta/^\circ$	$\gamma/^\circ$	$V/\text{Å}^3$
Exp. Data	11.125	17.922	21.228	97.356	94.354	90.218	4185
0 GPa	11.6923	21.1429	24.0634	99.8461	91.8269	90.0641	5857.9441
1.0 GPa	11.2534	17.9475	21.5008	97.1220	94.8802	90.0945	4293.0591
2.0 GPa	11.0823	17.2324	20.9940	96.4142	96.2508	90.1365	3960.1273
3.0 GPa	10.9812	16.8647	20.6702	96.1280	96.5726	90.2344	3780.6195
4.0 GPa	10.9060	16.5327	20.4201	95.7583	97.3946	90.3400	3632.1625
5.0 GPa	10.8451	16.2537	20.2224	95.5451	97.9829	90.4620	3512.7804
6.0 GPa	10.7895	15.9909	20.1035	95.2828	98.5488	90.5913	3414.4163
7.0 GPa	10.7315	15.7611	20.0150	95.1278	98.9668	90.6994	3329.4366
8.0 GPa	10.6729	15.5595	19.9380	95.0078	99.3458	90.7402	3253.3696
9.0 GPa	10.5365	15.3762	19.9136	94.8670	98.9342	90.9763	3174.0941
10.0 GPa	10.4930	15.1961	19.8954	94.8455	99.2521	90.8748	3118.5846

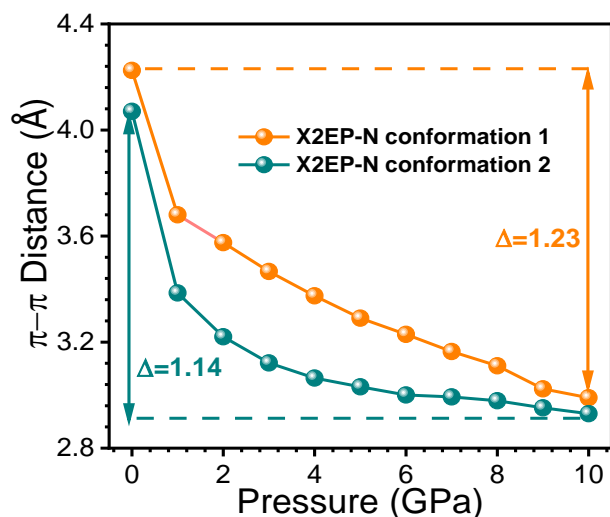


Figure S5. The changes of π - π distance with the increased pressure.

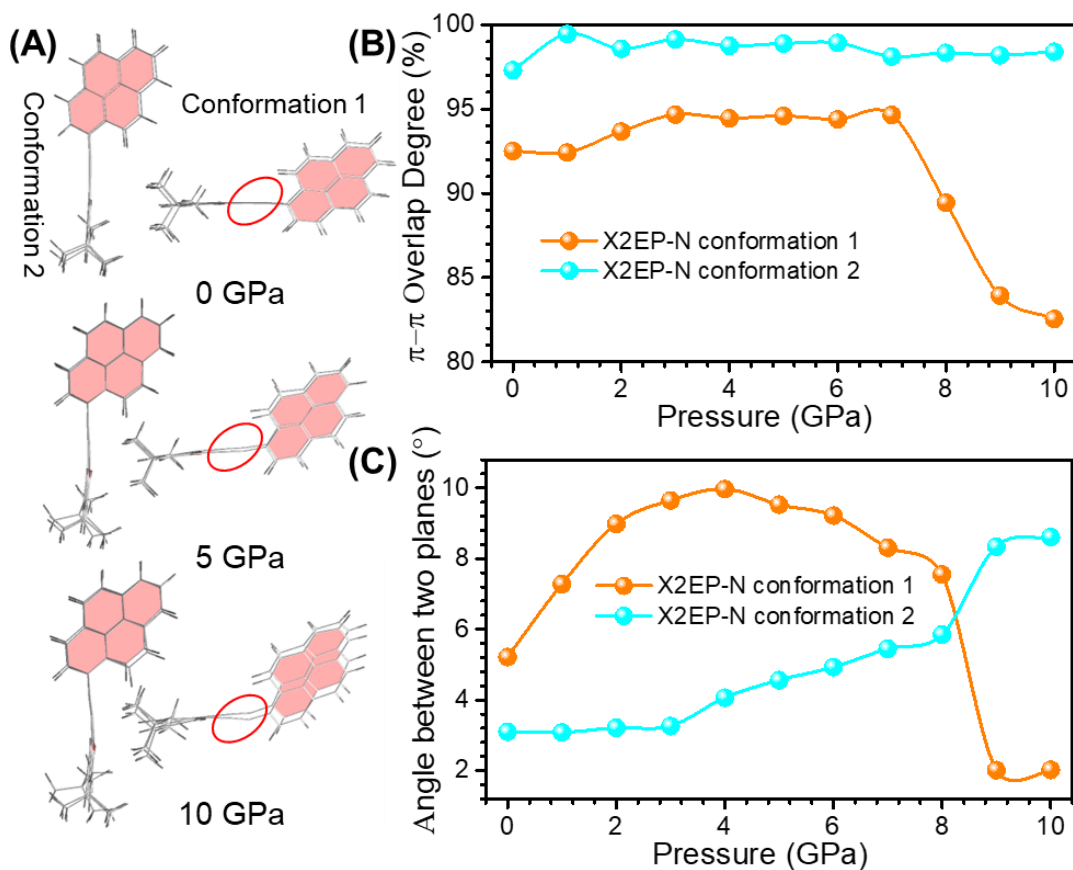


Figure S6. The analysis of π - π interactions including the overlap degree and angle between two pyrene planes of X2EP-N (two conformations) based on the calculated results: (A) photograph (The red circle represents the changes of alkyne group); variation trend of overlap degree (B) and angle (C) with the increased pressure.

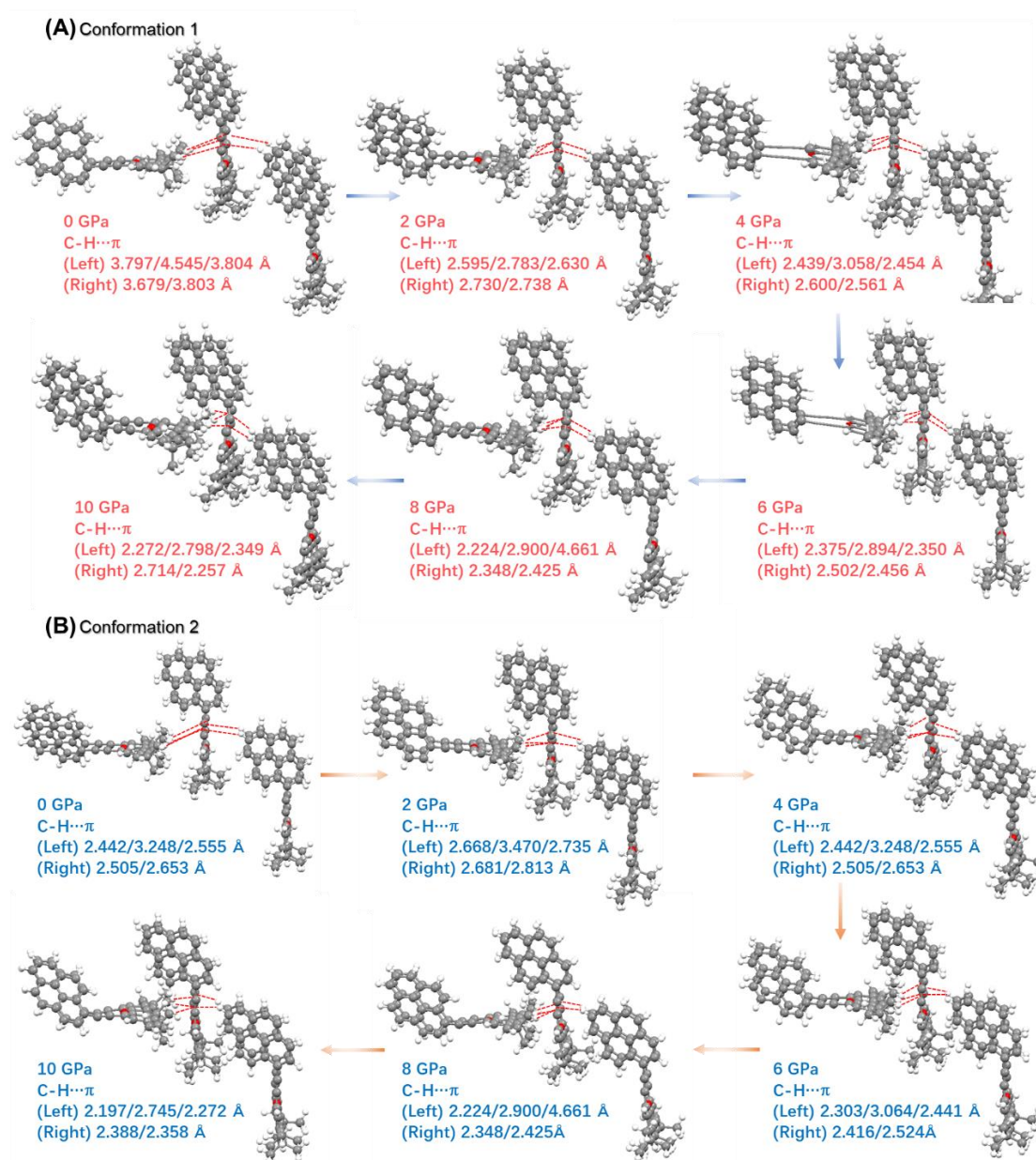


Figure S7. The analysis of intermolecular interactions (C-H... π) of X2EP-N-C1 and X2EP-N-C2 at different pressure values, which shows decreased tendency with the increased pressure.

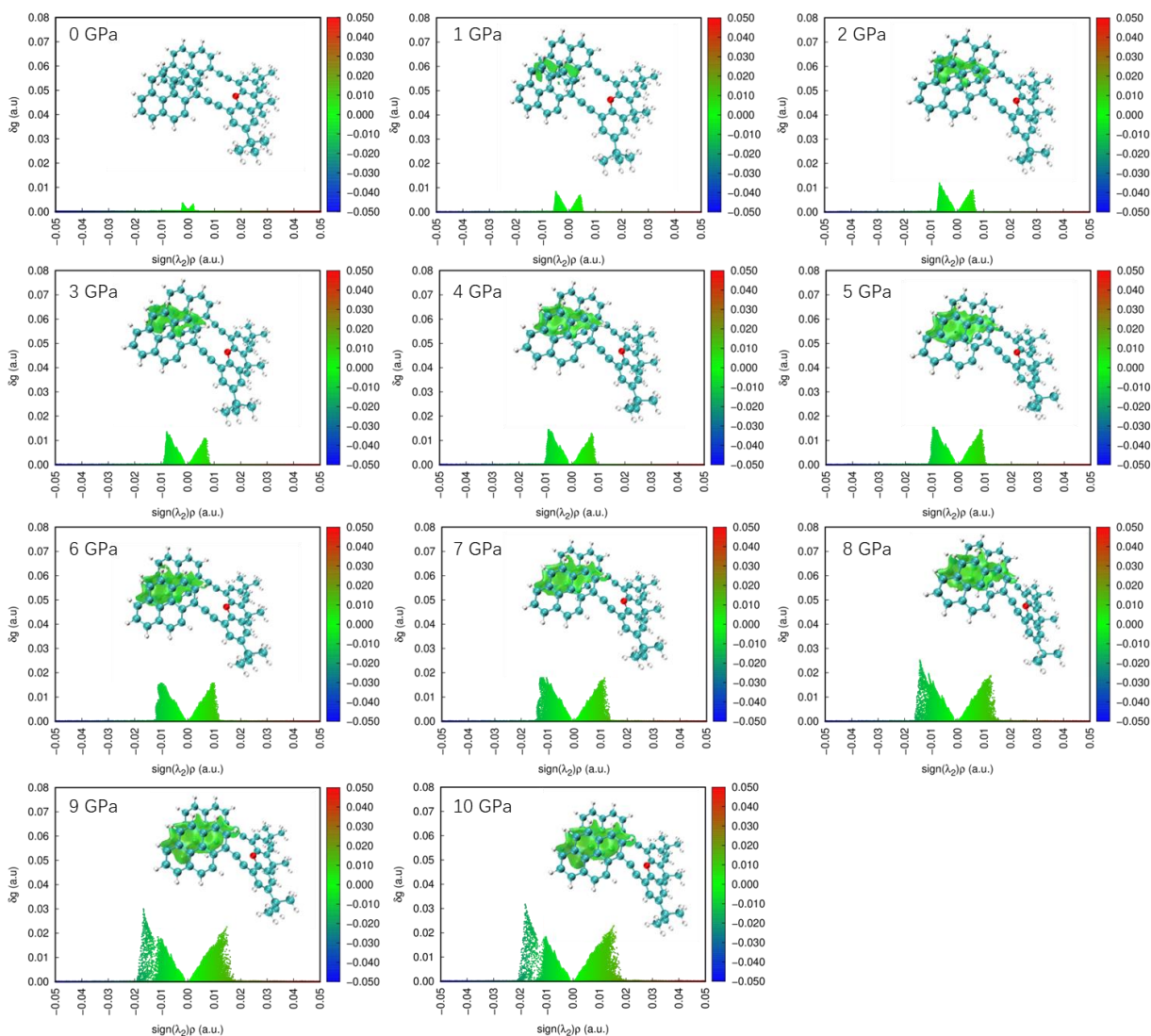


Figure S8. $\text{Sign}(\lambda_2)\rho$ colored isosurfaces of $\delta g_{\text{inter}} = 0.005$ a.u. and the corresponding scattering diagrams of X2EP-N-C1 corresponding to independent gradient model based on Hirshfeld partition (IGMH) analysis.

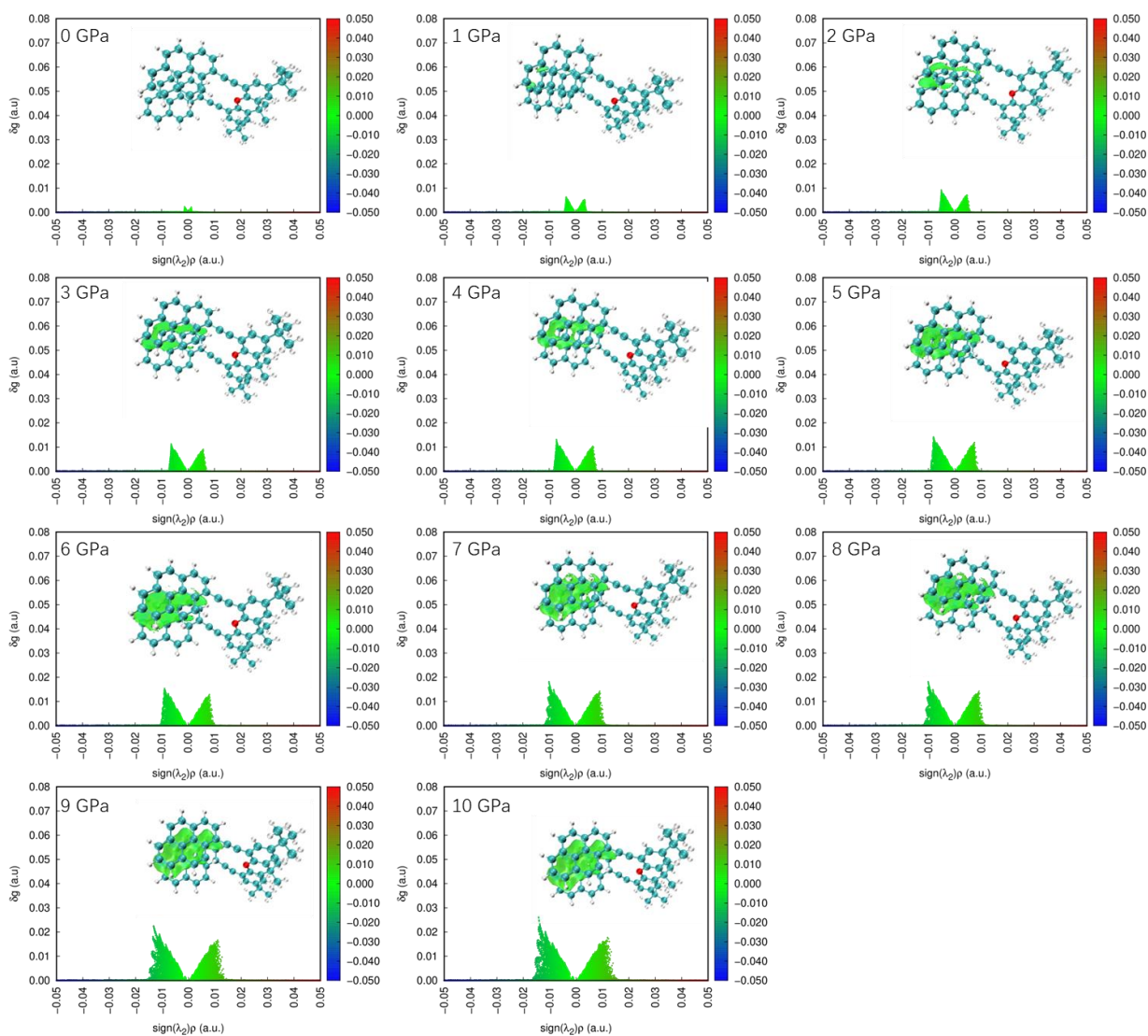


Figure S9. $\text{Sign}(\lambda_2)\rho$ colored isosurfaces of $\delta g_{\text{inter}} = 0.005$ a.u. and the corresponding scattering diagrams of X2EP-N-C2 corresponding to independent gradient model based on Hirshfeld partition (IGMH) analysis.

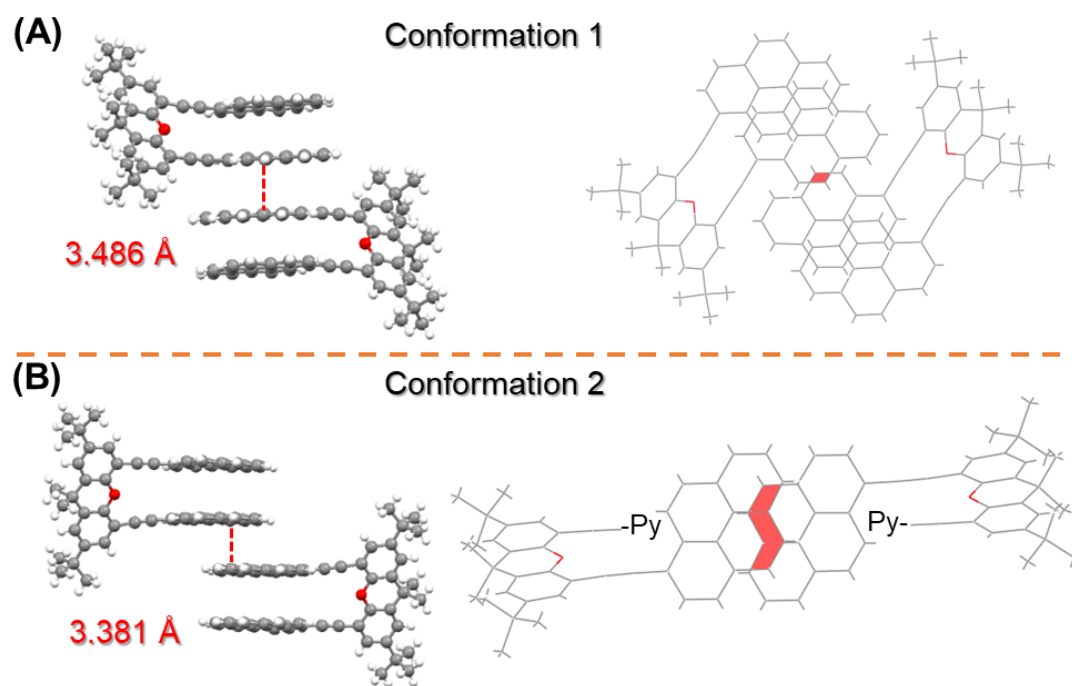


Figure S10. The π - π distance and overlap degree between two discrete dimers of X2EP-N-C1 (A) and X2EP-N-C2(B).

5. PL spectra of X2EP-B and X2EP-N during decompression process

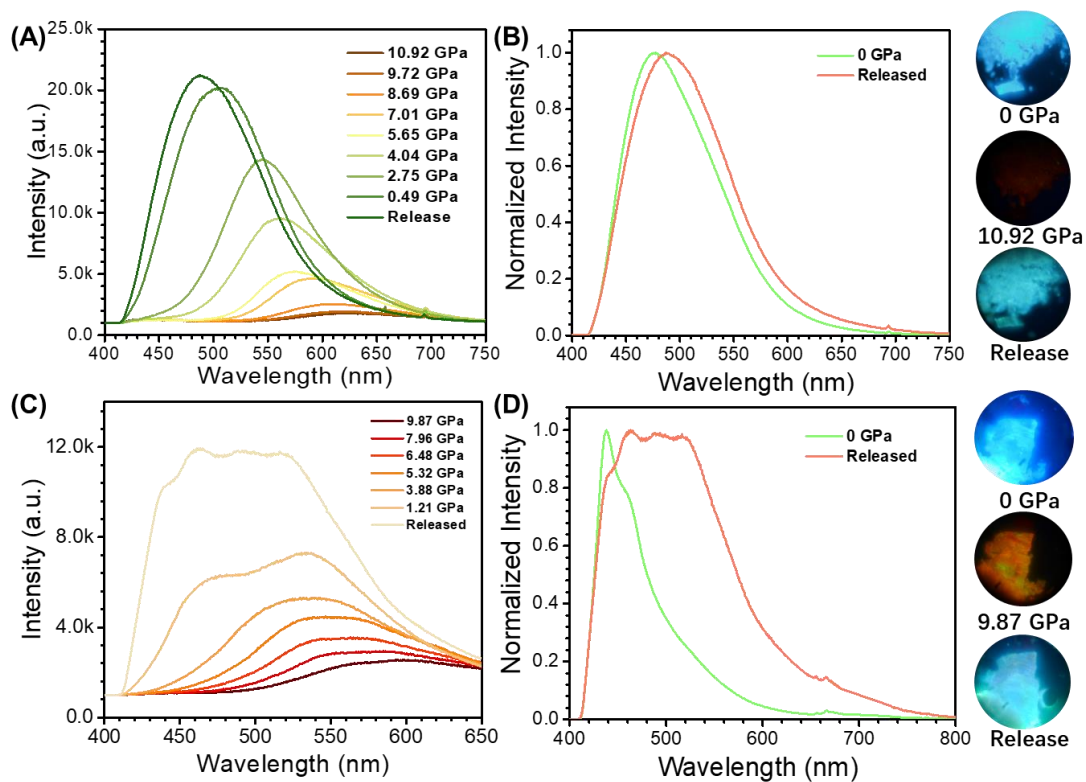


Figure S11. The PL spectra of X2EP-B (A) and X2EP-N (C) during the decompression process; The comparison between recovered and initial state of X2EP-B (B) and X2EP-N (D).

6. Analysis on π - π overlap and distance of X2EP-N

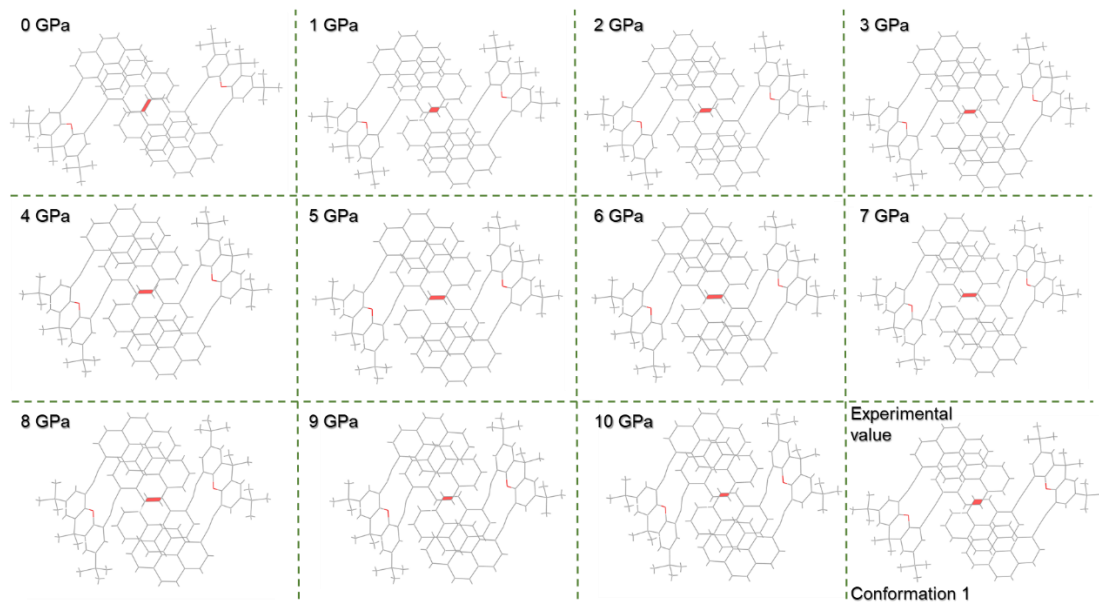


Figure S12. The changes of π - π overlap degree between two discrete dimers of X2EP-N-C1 at different pressure values.

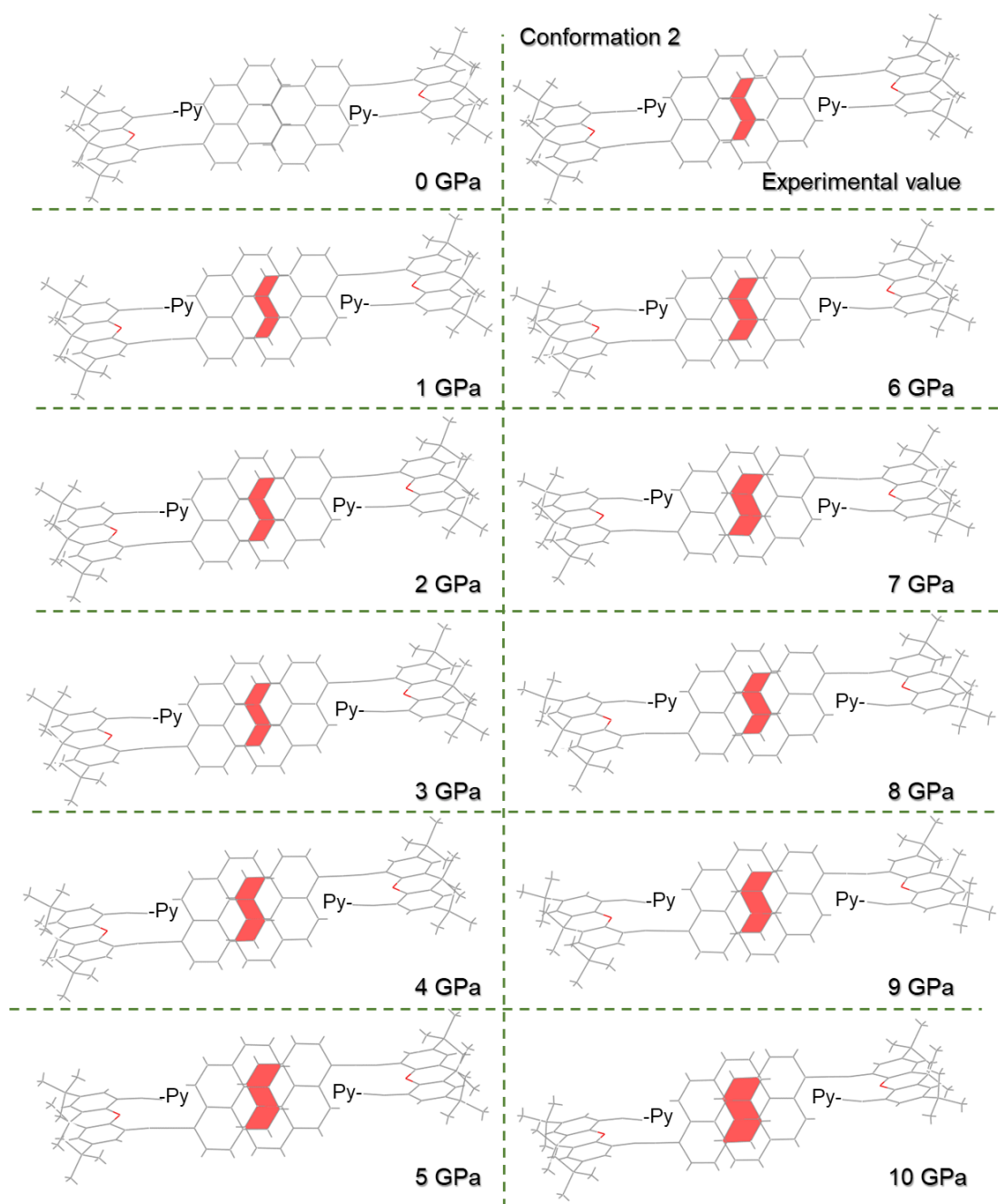


Figure S13. The changes of π - π overlap degree between two discrete dimers of X2EP-N-C2 at different pressure values. The atoms of another pyrene unit are deliberately hidden for the clear presentation of π - π overlap degree.

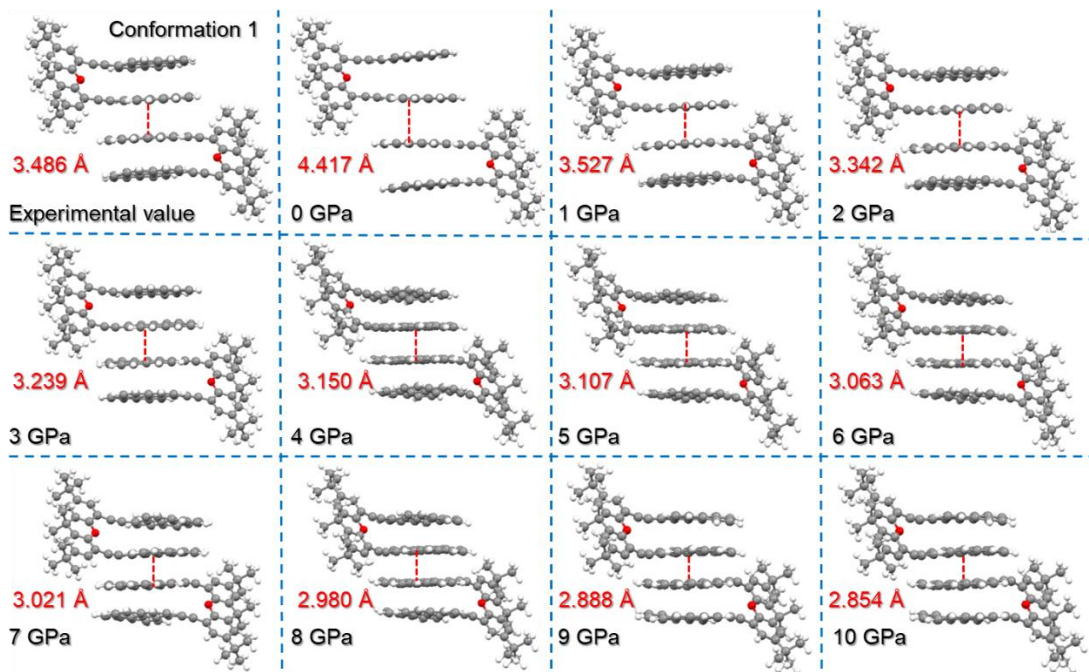


Figure S14. The changes of π - π distance between two discrete dimers of X2EP-N-C1 at different pressure values.

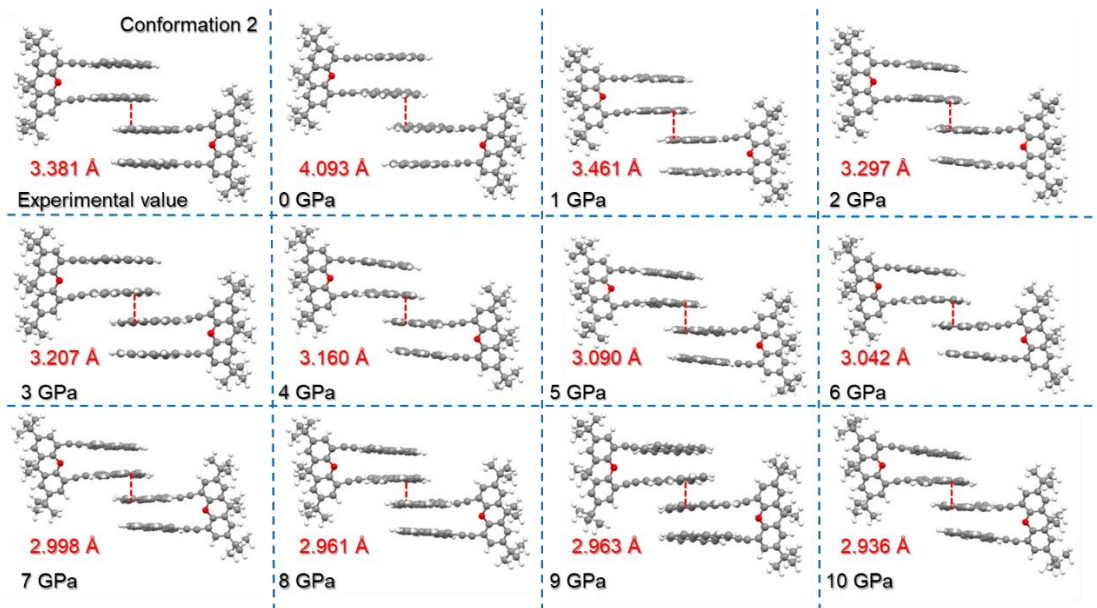


Figure S15. The changes of π - π distance between two discrete dimers of X2EP-N-C2 at different pressure values.

7. Analysis on stacking mode of Pyrene, X2P and X2EP-B.

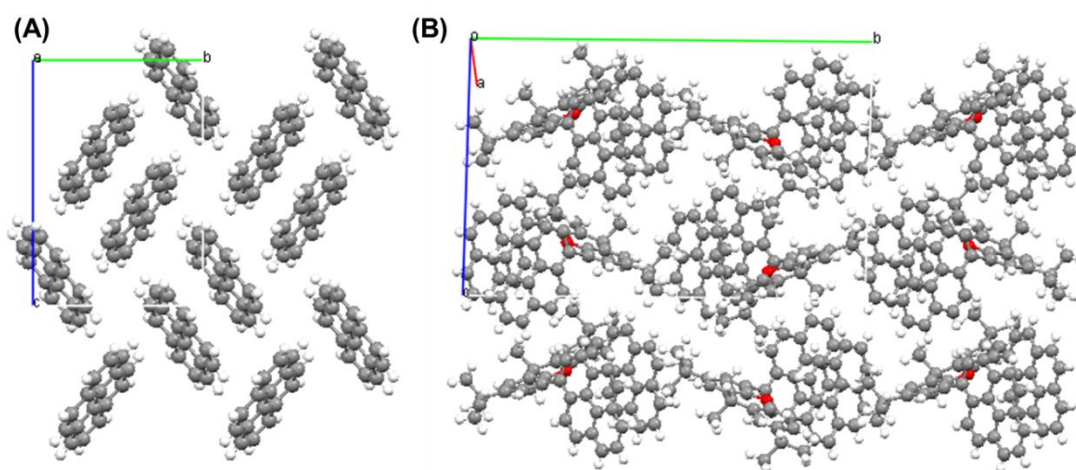


Figure S16. The stacking mode of Pyrene (A) and X2P (B) without tetramer.

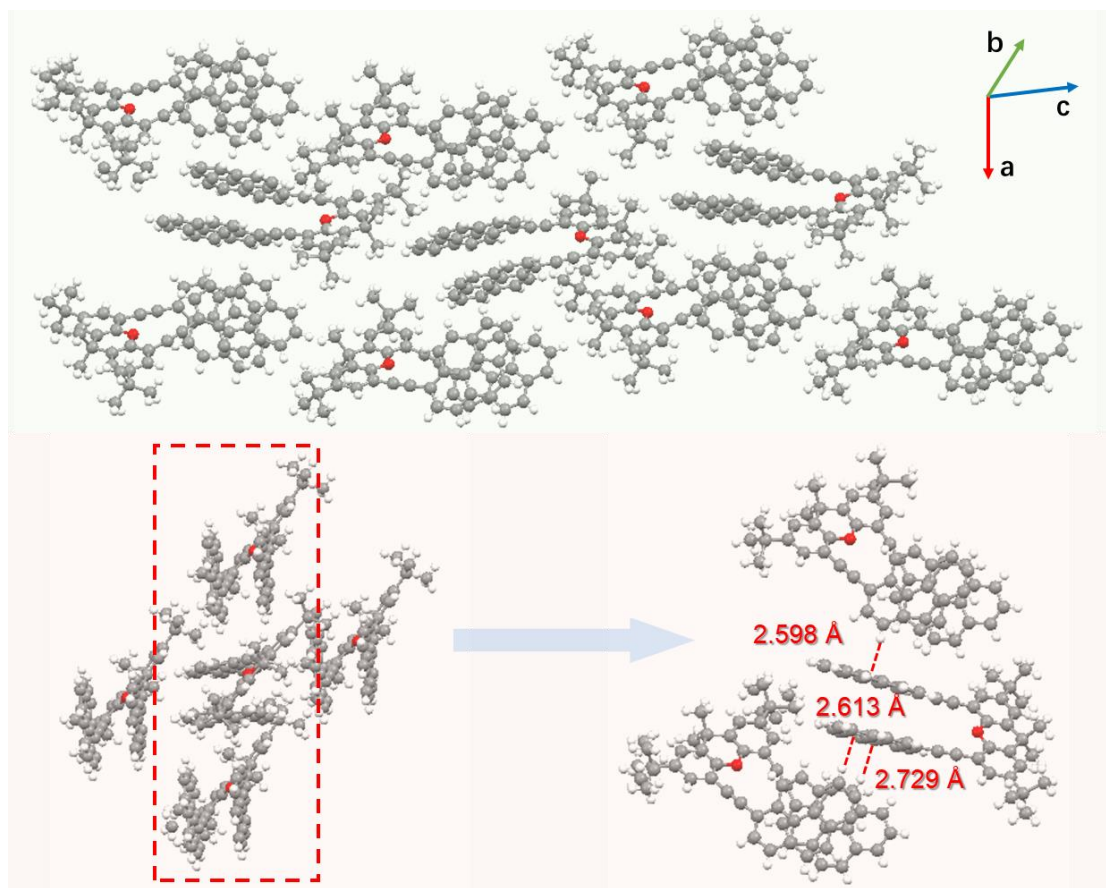


Figure S17. The analysis of stacking mode and intermolecular interactions (C-H... π) of X2EP-B without tetramer.

8. Lifetime of X2EP-N and X2EP-B.

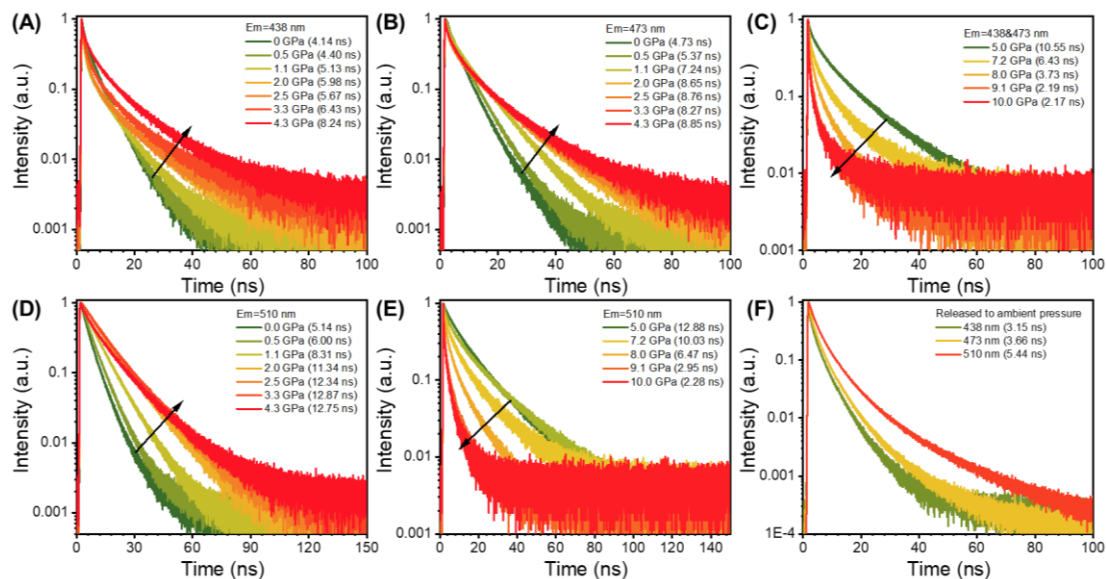


Figure S18. Time-resolved emission spectra of X2EP-N at 438 nm (A), 473 nm (B) and 510 nm (D) from 0 GPa to 4.3 GPa; Time-resolved emission spectra of X2EP-N at 438 nm&473 nm (C) and 510 nm (E) from 5.0 GPa to 10.0 GPa; Time-resolved emission spectra of X2EP-N when the pressure was released (F).

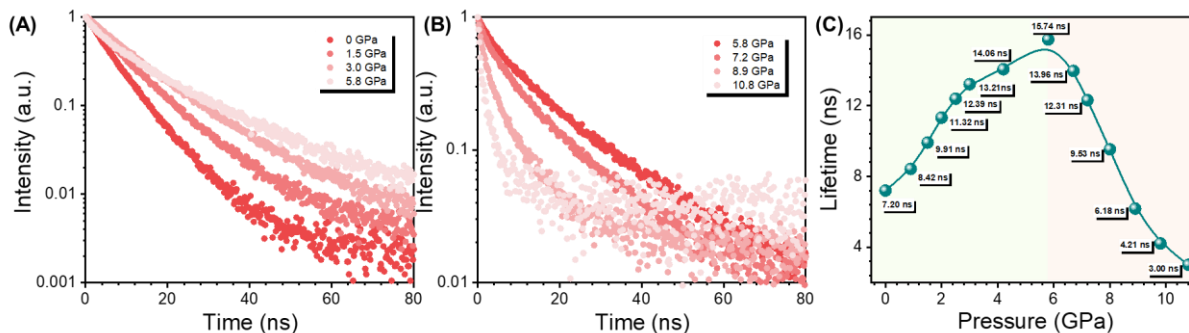


Figure S19. Time-resolved emission spectra of X2EP-B from 0 GPa to 5.8 GPa (A), from 5.8 GPa to 10.8 GPa (B); (C) Plot of lifetime against pressure for X2EP-B.

9. PL spectra of X2EP-N during the second compression.

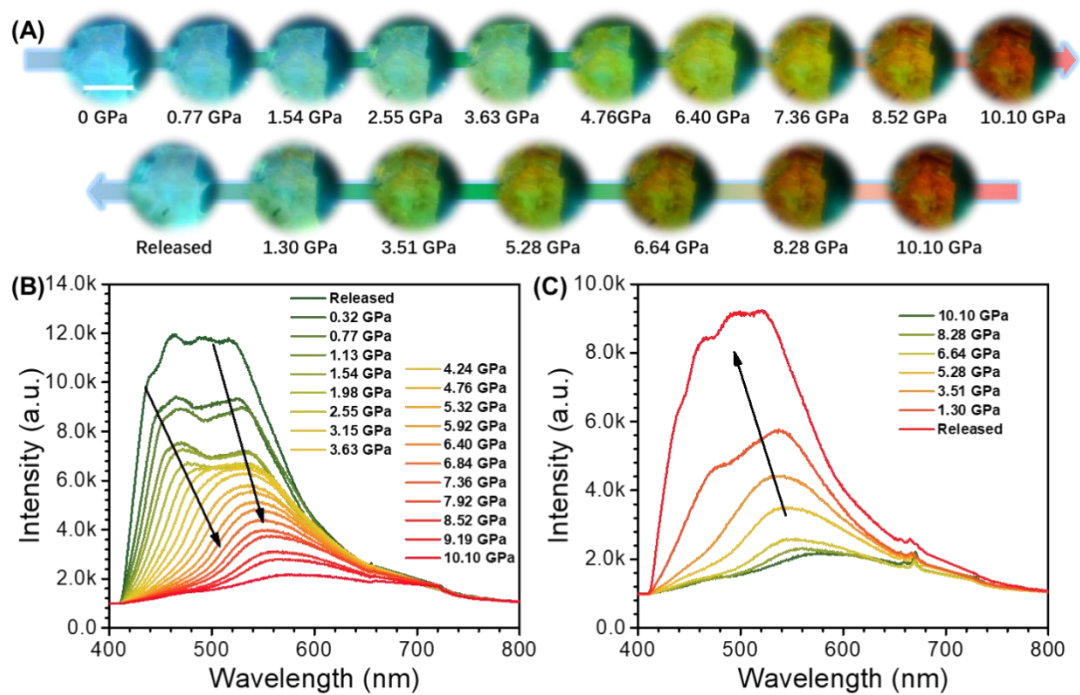


Figure S20. (A) The high-pressure fluorescence photographs X2EP-N during the second compression; The corresponding PL spectra of X2EP-N upon compression (B) and decompression (C). The scale is 100 μm , $\lambda_{\text{ex}}=365\text{ nm}$.

10. Absorption of X2EP-B and X2EP-N during compression process.

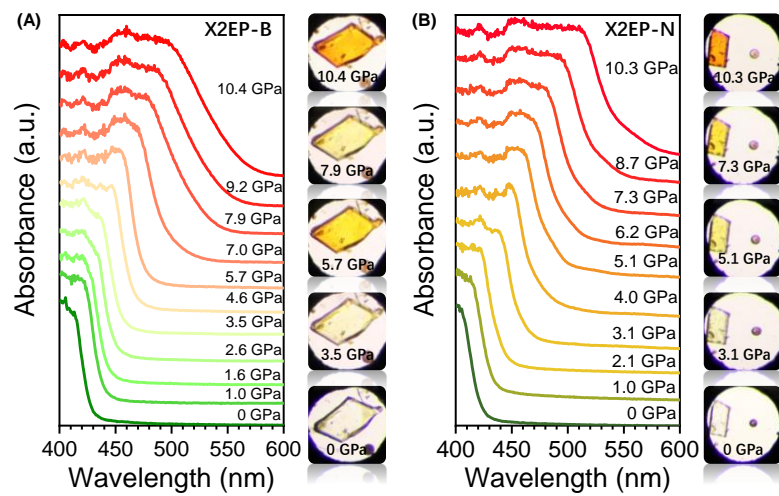


Figure S21. The high-pressure absorption spectra and corresponding optical photos of X2EP-B (A) and X2EP-N (B).

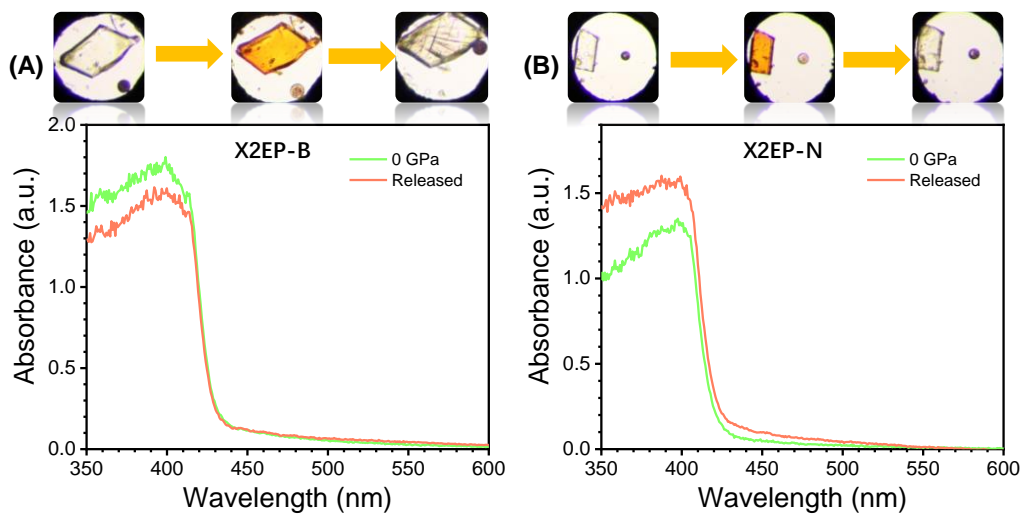


Figure S22. The comparison between the recovered spectrum and initial spectrum of X2EP-B (A) and X2EP-N (B).

11. References

- [1]. J. Wang, Q. Dang, Y. Gong, Q. Liao, G. Song, Q. Li, Z. Li, *CCS Chem.* 2021, 3, 274-286.
- [2]. T. Lu, F. Chen, *J. Comput. Chem.* 2012, 33, 580.
- [3]. C. Lefebvre, G. Rubez, H. Khartabil, J.-C. Boisson, J. ContrerasGarcía, E. Hénon, *Phys. Chem. Chem. Phys.* 2017, 19, 17928.
- [4]. T. Lu, Q. Chen, *J. Comput. Chem.* 2022, 43, 539-555.
- [5]. W. Humphrey, A. Dalke, K. Schulten, *J. Mol. Graphics* 1996,14, 33.